

## Electronic Supplementary Information

### Cucurbit[7]uril-driven modulation of ligand-DNA interactions by ternary assembly

Ekaterina Y. Chernikova,<sup>\*a</sup> Anna Y. Ruleva,<sup>a</sup> Vladimir B. Tsvetkov,<sup>b,c,d</sup> Yuri V. Fedorov,<sup>a</sup> Valentin V. Novikov,<sup>e</sup> Tseimur M. Aliyev,<sup>f</sup> Alexander A. Pavlov,<sup>e</sup> Nikolay E. Shepel<sup>a</sup> and Olga A. Fedorova<sup>\*a</sup>

<sup>a</sup> *Laboratory of Photoactive Supramolecular Systems, A.N. Nesmeyanov Institute of Organoelement Compounds of Russian Academy of Sciences, Russia, 119991, Moscow, Vavilova St. 28*

<sup>b</sup> *Computational oncology group, I.M. Sechenov First Moscow State Medical University, Trubetskaya str, 8/2, Moscow, 119146 Russia;*

<sup>c</sup> *Biophysics Department, Research and Clinical Center for Physical Chemical Medicine, Malaya Pirogovskaya str. 1a, Moscow 119435, Russia;*

<sup>d</sup> *Polyelectrolytes and Biomedical Polymers Laboratory, A.V. Topchiev Institute of Petrochemical Synthesis, Russian Academy of Sciences, Leninsky prospect str. 29, Moscow, 119991, Russia*

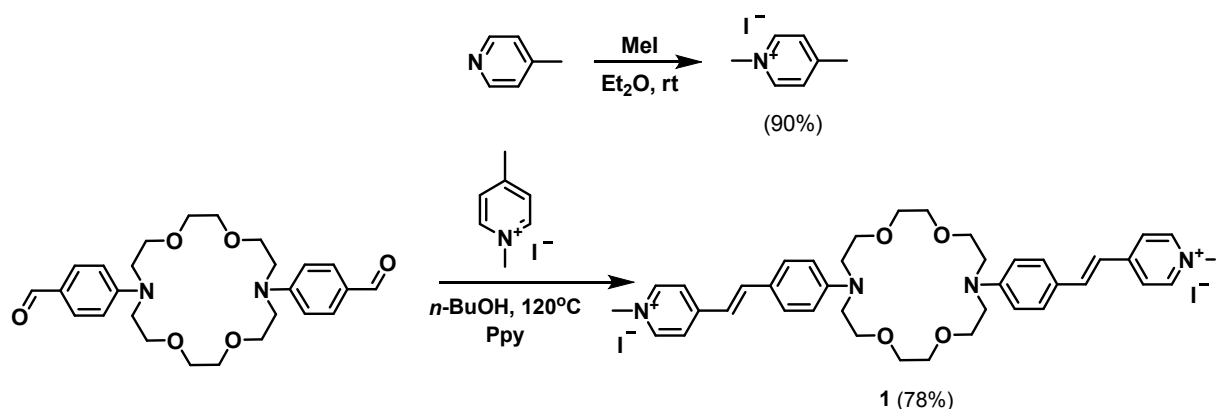
<sup>e</sup> *Laboratory of Nuclear Magnetic Resonances, A.N. Nesmeyanov Institute of Organoelement Compounds of Russian Academy of Sciences, Russia, 119991, Moscow, Vavilova St. 28*

<sup>f</sup> *Center for molecule composition studies, A.N. Nesmeyanov Institute of Organoelement Compounds of Russian Academy of Sciences, Russia, 119991, Moscow, Vavilova St. 28*

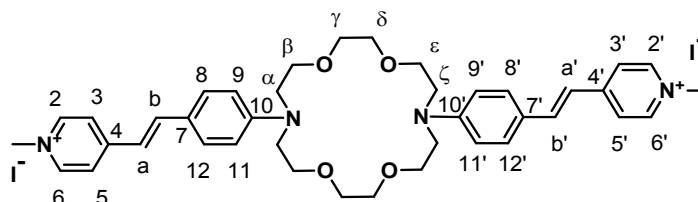
<b>Table of contents</b>	<b>Pages</b>
1. Synthesis and characterization	2
2. Optical spectroscopy data	3
3. Molecular modeling data	5
4. NMR spectroscopy data	8
5. References	13

## 1. Synthesis and characterization

1,4-Dimethylpyridinium iodide was prepared according to literature procedures.<sup>1</sup>



**4,4'-(1E,1'E)-2,2'-(4,4'-(1,4,10,13-tetraoxa-7,16-diazacyclooctadecane-7,16-diyl)bis(4,1-phenylene))bis(ethene-2,1-diyl)bis(1-methylpyridinium) iodide (L)**



1,4-Dimethylpyridinium iodide (62.4 mg, 0.27 mmol) and 4,4'-dibenzaldehyde-diaza-18-crown-6 ether (50 mg, 0.11 mmol) were dissolved in *n*-BuOH (5 mL) with addition of piperidine (0.04 mL). The mixture was stirred at 120 °C under argon during 11.5 h. The reaction mixture was cooled to -10 °C, and the precipitate was filtered off, thoroughly washed with hot benzene and dried in air. Dye **1** was obtained as dark red crystals in 78% yield (75 mg, 0.08 mmol). Mp. 209–211 °C with decomposition, <sup>1</sup>H NMR (400 MHz; DMSO-*d*<sub>6</sub>): 3.61-3.52 (br.s, 8H, H- $\alpha$ , H- $\zeta$ ), 3.71-3.61 (br.s, 16H, H- $\beta$ , H- $\gamma$ , H- $\delta$ , H- $\epsilon$ ), 4.16 (s, 6H, 2CH<sub>3</sub>), 6.78 (d, 4H, H-9, H-9', H-11, H-11', *J* = 8.9), 7.13 (d, 2H, H-a, H-a', *J*<sub>trans</sub> = 16.1), 7.56 (d, 4H, H-8, H-8', H-12, H-12', *J* = 8.9), 7.88 (d, 2H, H-b, H-b', *J*<sub>trans</sub> = 16.1), 8.03 (d, 4H, H-3, H-3', H-5, H-5', *J* = 6.8), 8.68 (d, 4H, H-2, H-2', H-6, H-6', *J* = 6.8). <sup>13</sup>C NMR (126 MHz, DMSO-*d*<sub>6</sub>,  $\delta$  M.D.): 46.38 (2C, CH<sub>3</sub>), 50.59 (4C, C- $\alpha$ , C- $\zeta$ ), 68.14 (4C, H- $\beta$ , H- $\epsilon$ ), 70.26 (4C, H- $\gamma$ , H- $\delta$ ), 111.67 (4C, C-9, C-9', C-11, C-11'), 117.05 (2C, C-a, C-a'), 122.13 (4C, C-3, C-3', C-5, C-5'), 122.41 (2C, C-7, C-7'), 130.43 (4C, C-8, C-8', C-12, C-12'), 141.78 (2C, C-b, C-b'), 144.35 (4C, C-2, C-2', C-6, C-6'), 149.89 (2C, C-10, C-10'), 153.37 (2C, C-4, C-4'). Anal. calcd. for C<sub>40</sub>H<sub>50</sub>N<sub>4</sub>I<sub>2</sub>O<sub>4</sub>: C, 53.11; H, 5.57; N, 6.19; found: C, 52.61; H, 5.58; N, 6.22. ESI-MS **1** in H<sub>2</sub>O, *m/z*: found [1]<sup>2+</sup> 325.20 for C<sub>40</sub>H<sub>50</sub>N<sub>4</sub>O<sub>4</sub><sup>2+</sup> calcd. 325.19.

## 2. Optical spectroscopy data

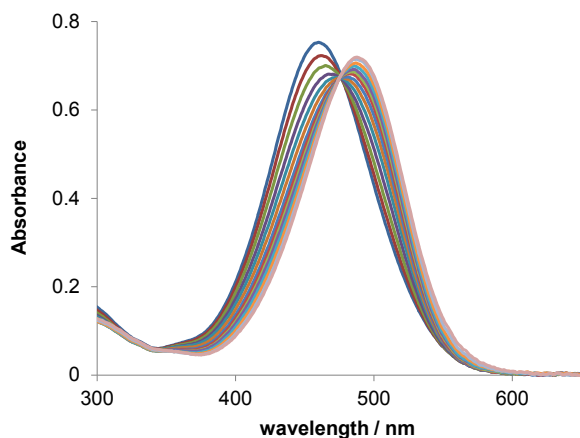


**Figure S1.** UV-Vis spectra of bis-styryl dye ( $1.5 \times 10^{-5}$  M) with increasing CB[7] concentration ( $0-1.2 \times 10^{-3}$  M),  $H_2O$ .

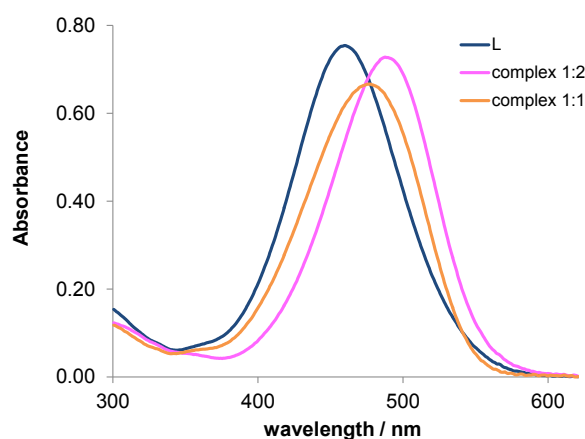


**Figure S2.** Electronic absorption spectra obtained by a global fit of the spectrophotometric titration data using the SpecFit/32 program for bis-styryl dye (blue curve) and its complexes dye-CB[7] (orange curve) and dye-(CB[7])<sub>2</sub> (pink curve),  $H_2O$ .

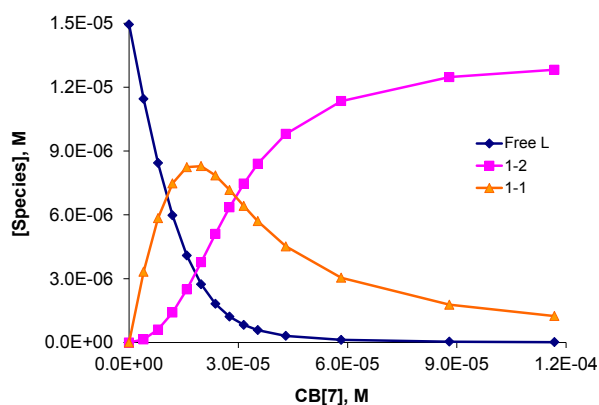


**Figure S3.** Concentrations of the solution components: bis-styryl dye (blue curve) and its complexes dye-CB[7] (orange curve) and dye-(CB[7])<sub>2</sub> (pink curve), depending on the CB[7] concentration,  $H_2O$ .

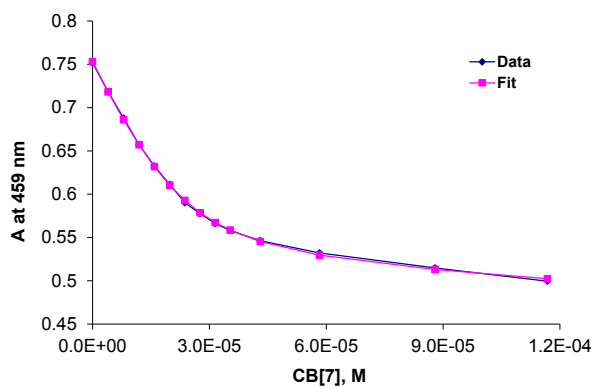


**Figure S4.** Changes in absorption spectra of bis-styryl dye at 459 nm depending on the CB[7] concentration: experimental data and obtained by a global fit of the spectrophotometric titration data using the SpecFit/32 program, H<sub>2</sub>O.

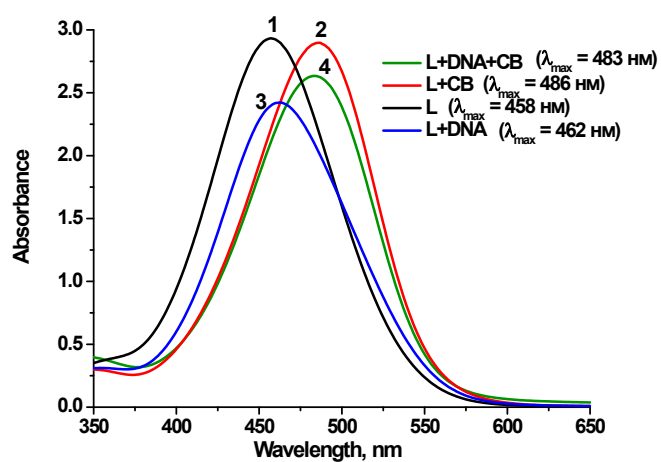


**Figure S5.** Absorption spectra of free L and in the presence of DNA and/or CB[7]: (1)  $C_L = 6 \cdot 10^{-5}$  M (black); (2)  $C_{CB[7]} = 6 \cdot 10^{-4}$  M,  $C_L = 6 \cdot 10^{-5}$  M (red); (3)  $C_{DNA} = 10^{-4}$  M,  $C_L = 6 \cdot 10^{-5}$  M (blue); (4)  $C_{CB[7]} = 6 \cdot 10^{-4}$  M,  $C_L = 6 \cdot 10^{-5}$  M,  $C_{DNA} = 10^{-4}$  M (green).

### 3. Molecular modeling data

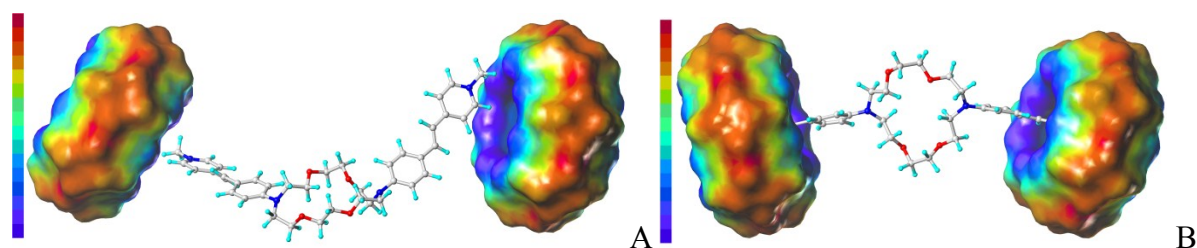


**Figure S6.** Snapshots of arrangement of dye and cucurbiturils molecules relative to each other. (A) – the starting position of components, (B) - after 14 picoseconds MD simulations. The cucurbiturils are covered with a Connolly surface, which is colored depending on the distribution of the electrostatic potential from negative (blue) to positive (red).

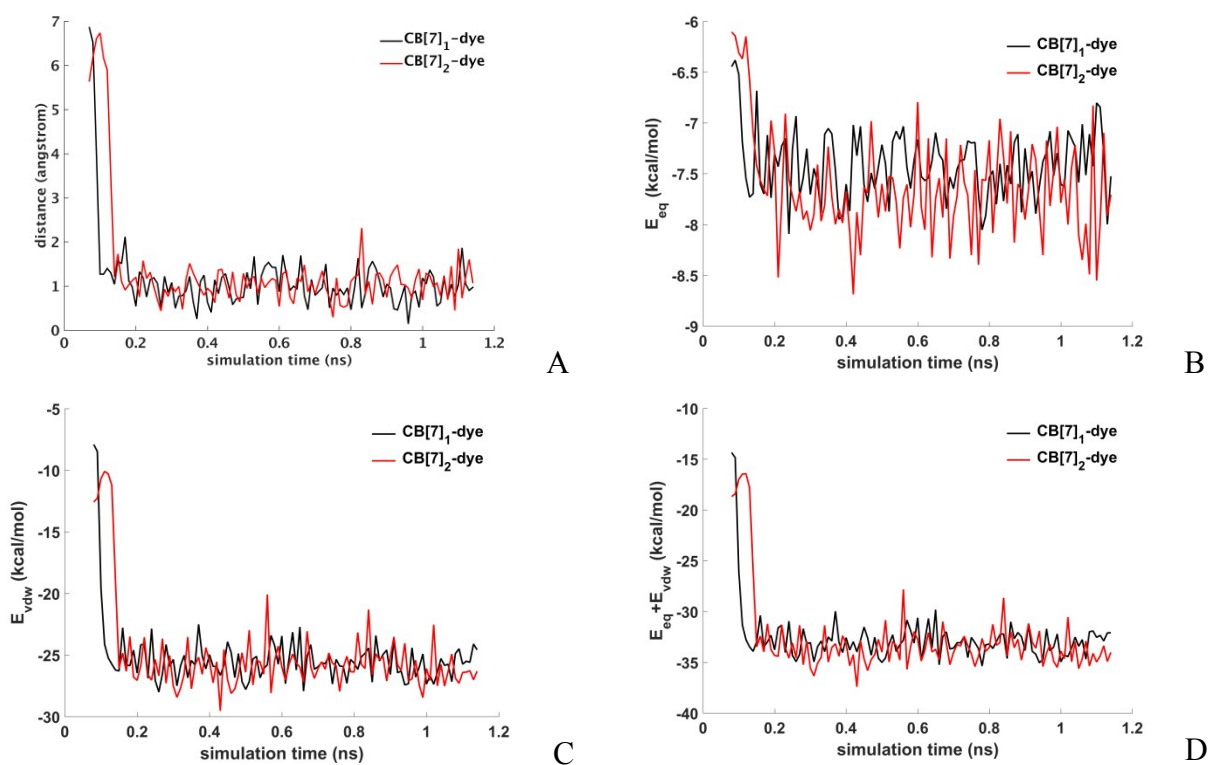


**Figure S7.** The evolution of the distance between pyridinium N-atom of dye and center of carbonyl portal of CB[7] farthest from this N-atom (A). Evolution of the Coulomb ( $E_{eq}$ ) (B), van der Waals ( $E_{vdw}$ ) (C) and their sum ( $E_{eq} + E_{vdw}$ ) (D) contributions to the interaction energy of bis-styryl dye with one (black) or two (red) CB[7] molecules.

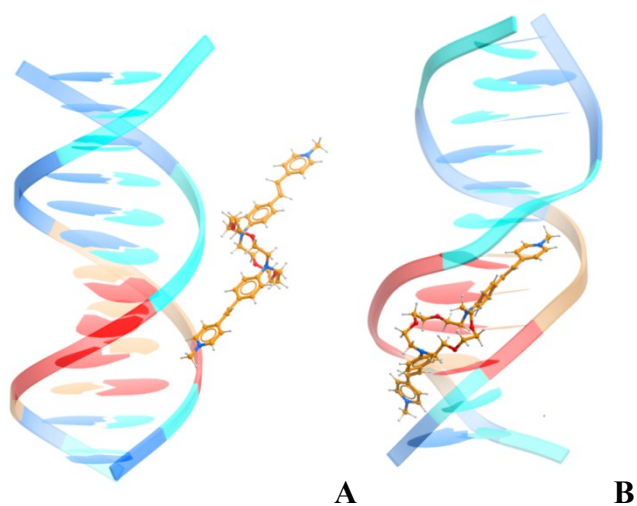


**Figure S8.** Snapshots of arrangement of dye and DNA molecules relative to each other. (A) – the starting position of components, (B) - after 38 nanoseconds MD simulation.

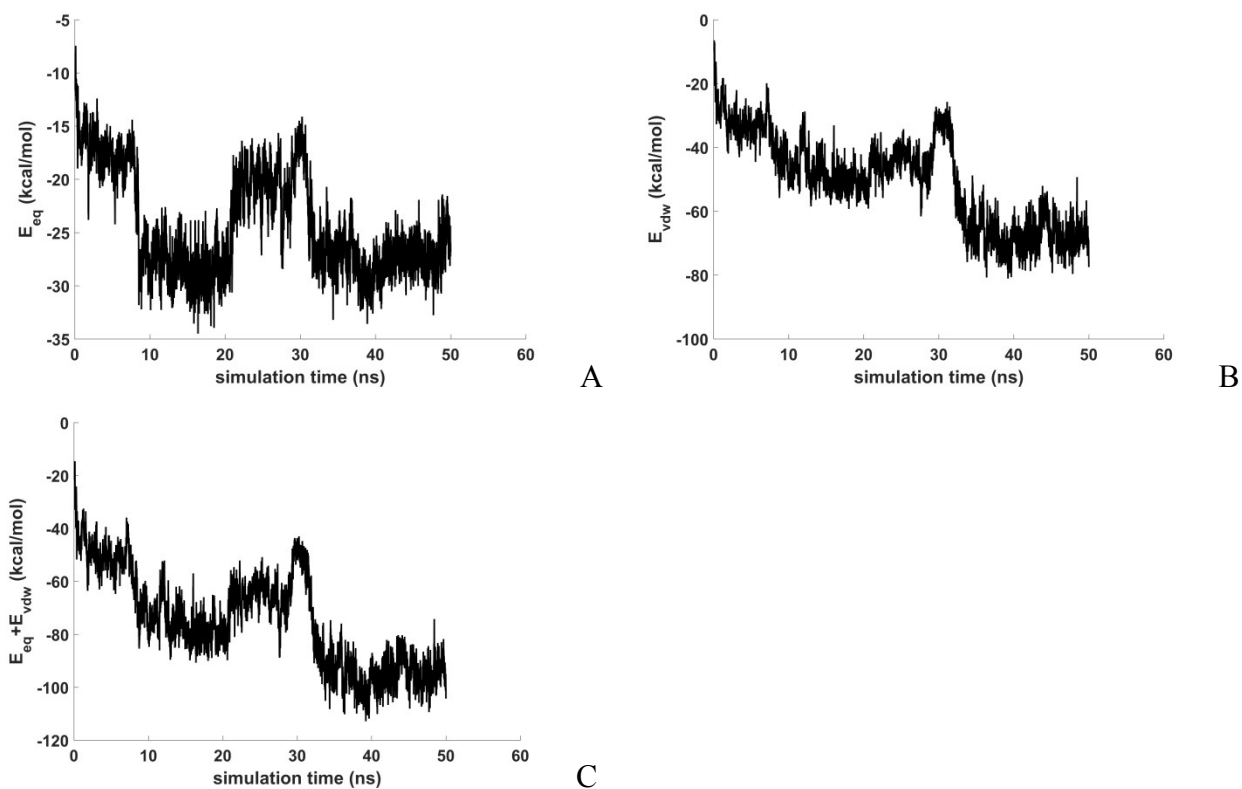


**Figure S9.** Evolution of the Coulomb ( $E_{eq}$ ) (A), van der Waals ( $E_{vdw}$ ) (B) and their sum ( $E_{eq} + E_{vdw}$ ) (C) contributions to the interaction energy of bis-styryl dye with DNA.

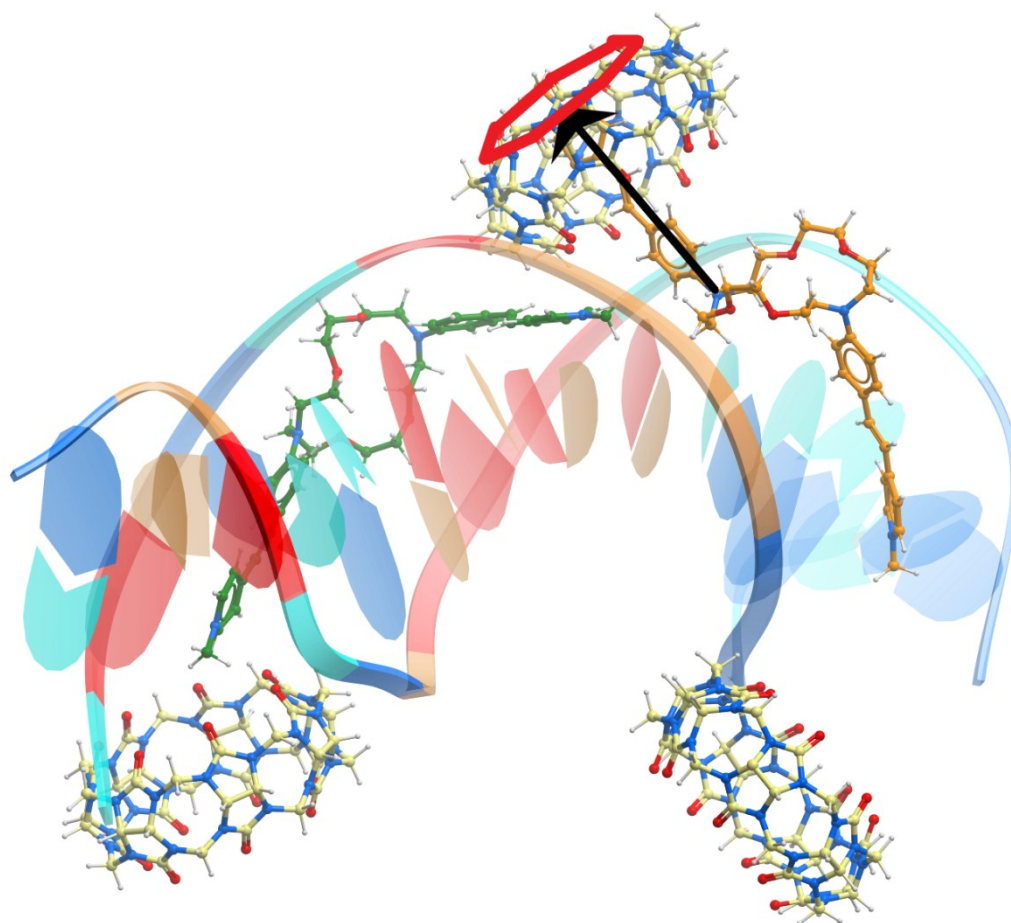


**Figure S10.** Locations of the DNA, bis-styryl dye and cucurbiturils in the final stages of MD calculations: A - start, B - final. The DNA shown by rendering with the nucleotides colored as follows: G - blue, A - red, T - light brown, C - cyan. Atoms are represented by the following colors: cucurbituril carbon - yellow, bis-styryl dye carbon - beige and green, oxygen - red, nitrogen - blue, hydrogen - white. A black vector is a vector connecting the aliphatic and pyridinium N-atoms of dye molecule. The red closed line marks the plane of carbonyl portal of CB[7].

#### 4. NMR spectroscopy data

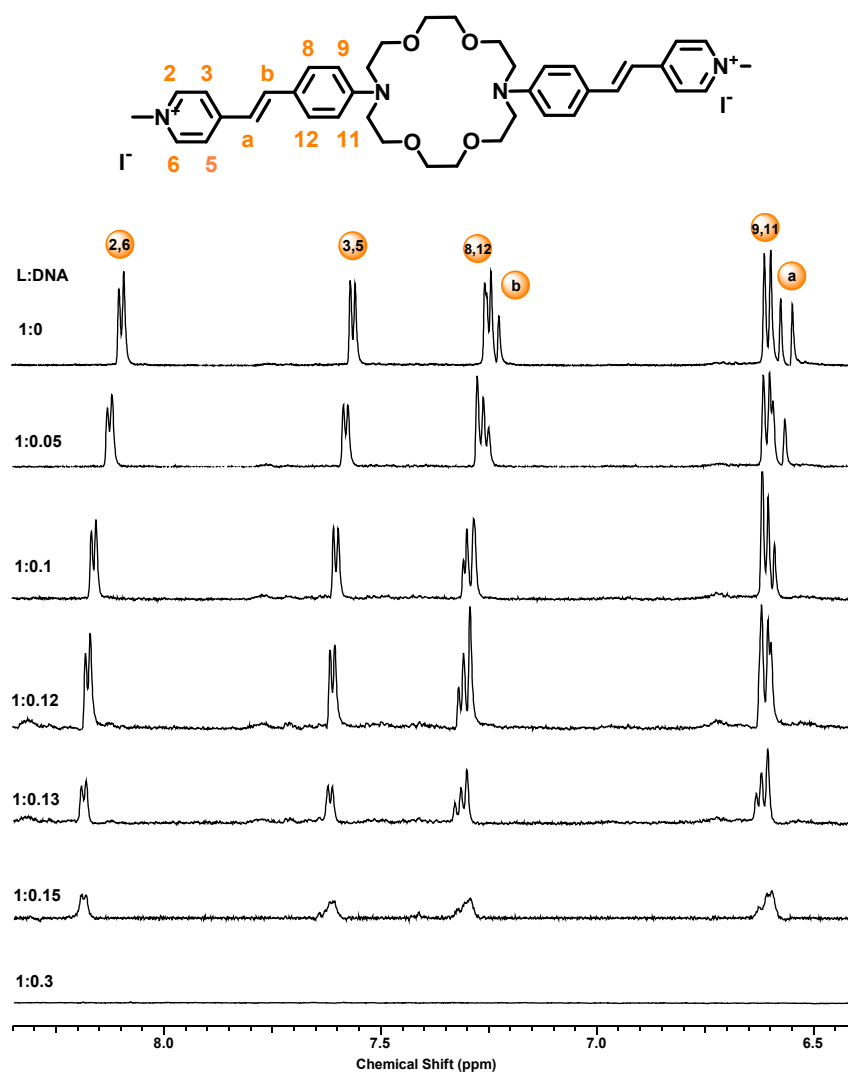


**Figure S11.** Aromatic part of  $^1\text{H}$  NMR spectra (600 MHz, 298 K, sodium phosphate buffer/ $\text{D}_2\text{O}$  9:1, 1mM) of free ligand **L** and in the presence of different amounts of Dickerson dodecamer.



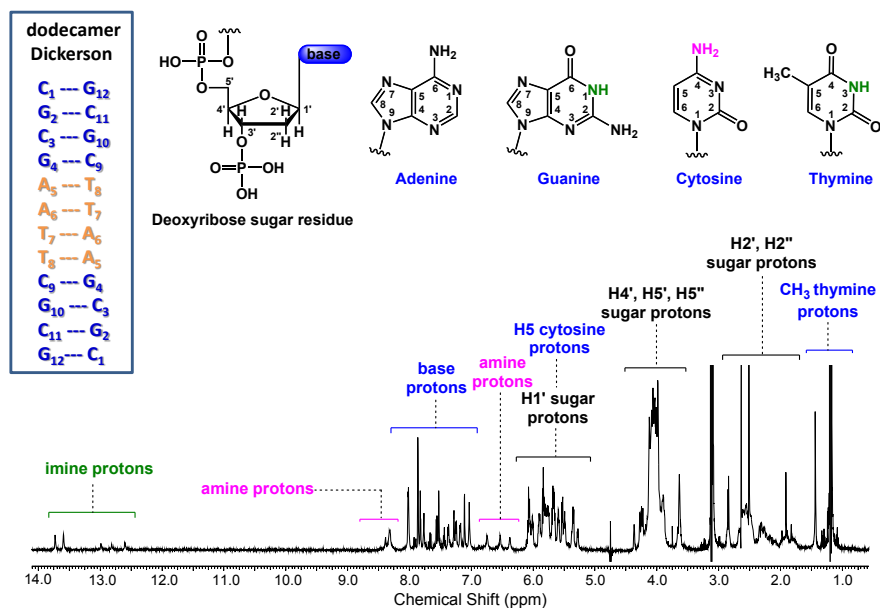


**Figure S12.** Assignment of dodecamer Dickerson protons. Green and pink color display visible exchangeable protons such as NH of guanines and thymines and NH<sub>2</sub> of cytosines.

**Table S1.** Assignment of the <sup>1</sup>H NMR spectrum of the oligonucleotide d(CGCGAATTCGCG)<sub>2</sub> in D<sub>2</sub>O.

Residue	C8H	C6H	C5H	C2H	CH3	C1'H	C2'H/C2''H	C4'H
C1		7.56	5.84			5.68	2.27/1.85	4.15
G2	7.86					5.79	2.56/2.52	4.31
C3		7.17	5.28			5.49	2.13/1.7	4.17
G4	7.77					5.38	2.63/2.52	4.29
A5	8.02			7.11		5.90	2.82/2.57	4.44
A6	8.02			7.53		6.05	2.79/2.42	4.44
T7		7.03			1.20	5.82	2.42/1.87	4.24
T8		7.28			1.44	6.01	2.44/2.05	4.24
C9		7.37	5.53			5.59	2.30/1.94	4.20
G10	7.82					5.76	2.56/2.52	4.35
C11		7.24	5.35			5.66	2.19/1.79	4.20
G12	7.86					6.08	2.50/2.23	4.20

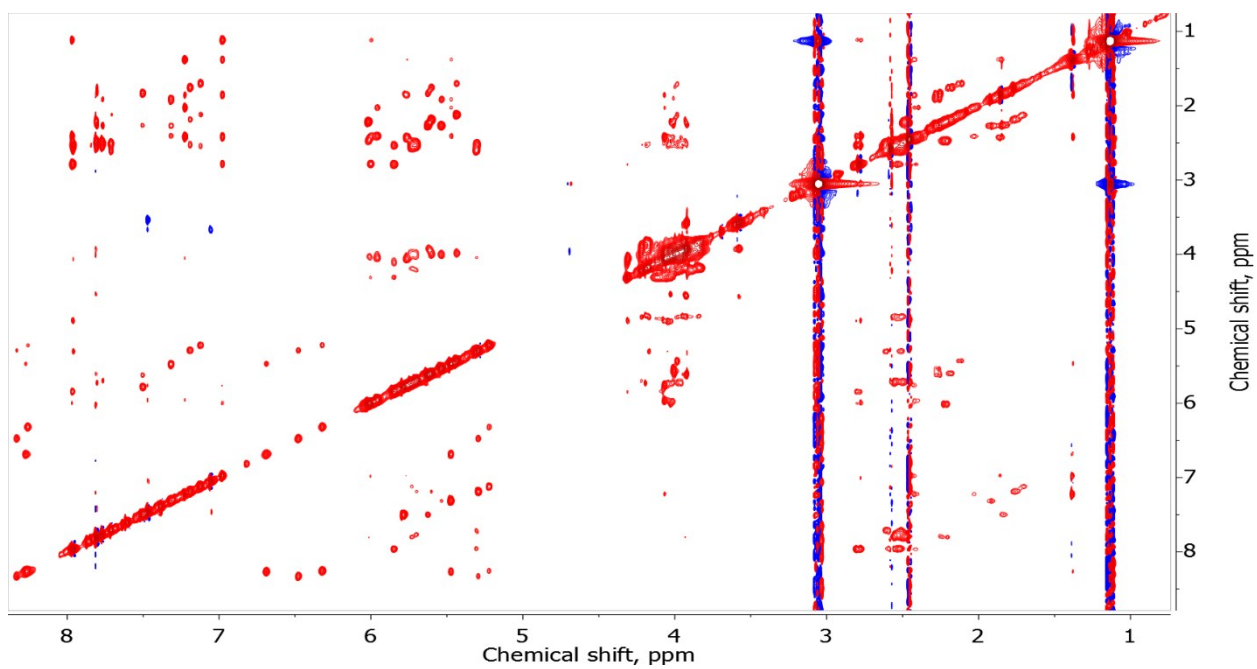


**Figure S13.** 600 MHz NOESY of 1mM DD in 10mM phosphate buffer:D<sub>2</sub>O 9:1 (pH=7.0).

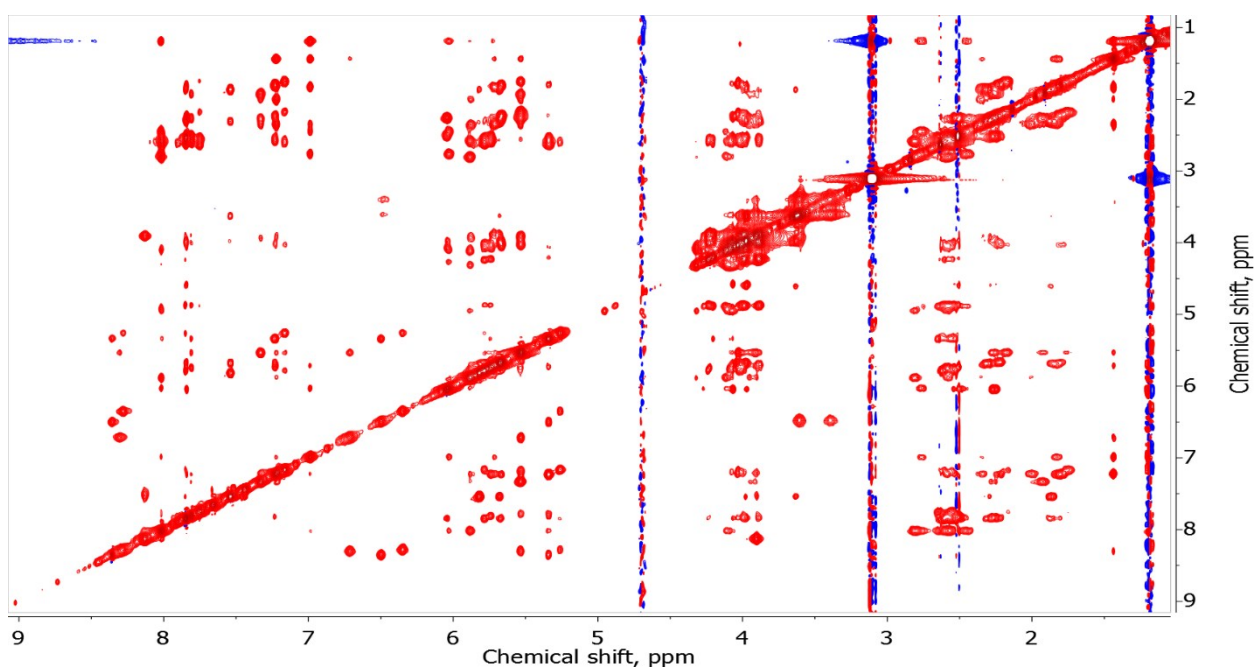


**Figure S14.** 600 MHz NOESY of L-DD (0.3-1) mixture in 10mM phosphate buffer:D<sub>2</sub>O 9:1 (pH=7.0).

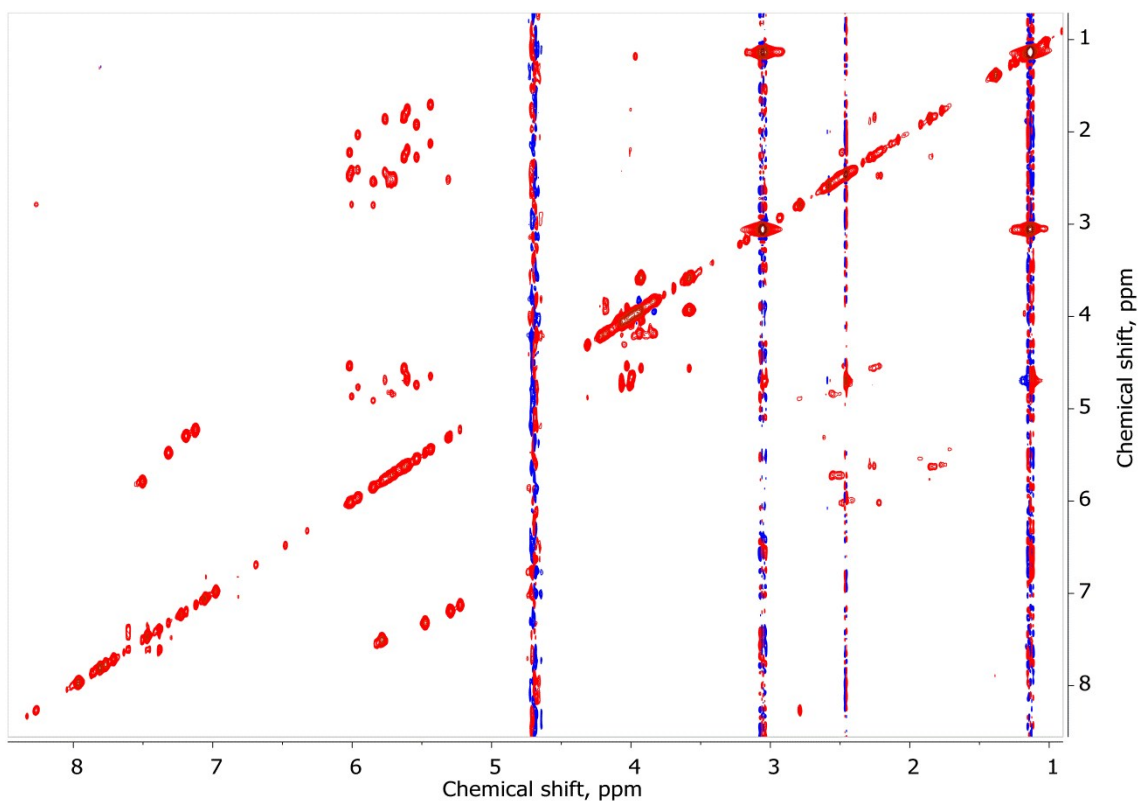


**Figure S15.** 600 MHz TOCSY of 1mM DD in 10mM phosphate buffer:D<sub>2</sub>O 9:1 (pH=7.0).

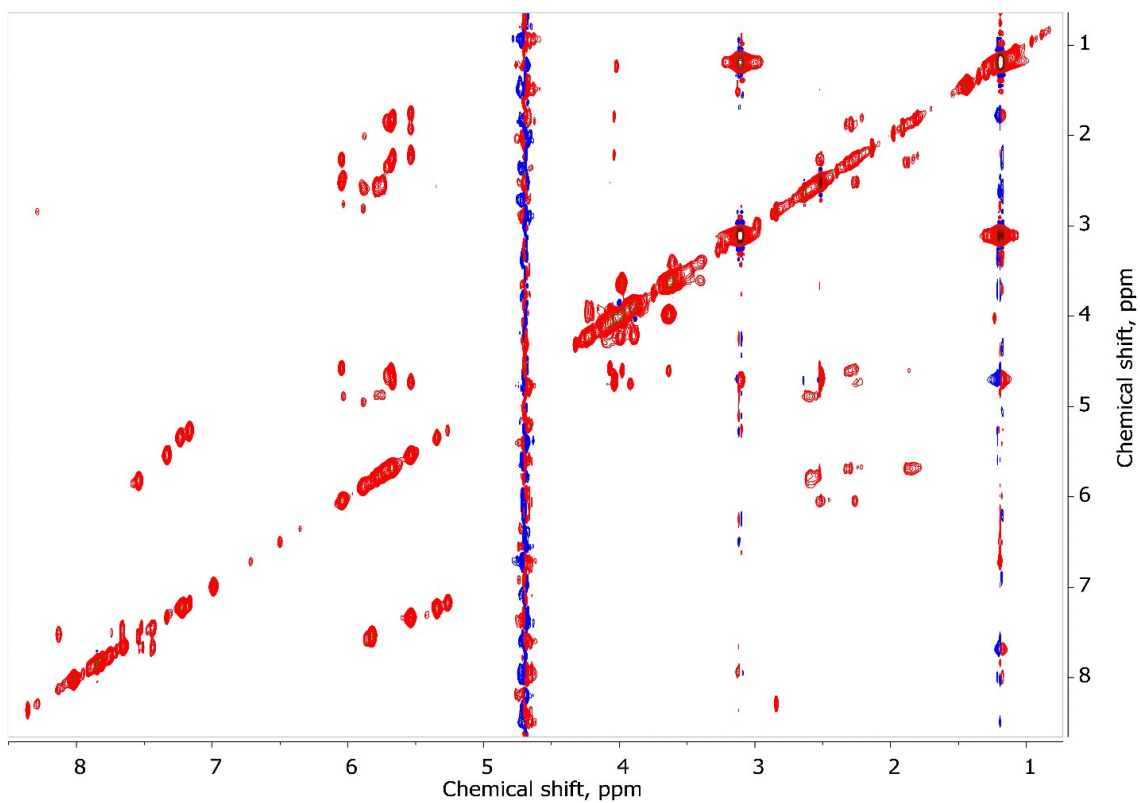


**Figure S16.** 600 MHz TOCSY of L-DD (0.3-1) mixture in 10mM phosphate buffer:D<sub>2</sub>O 9:1 (pH=7.0).

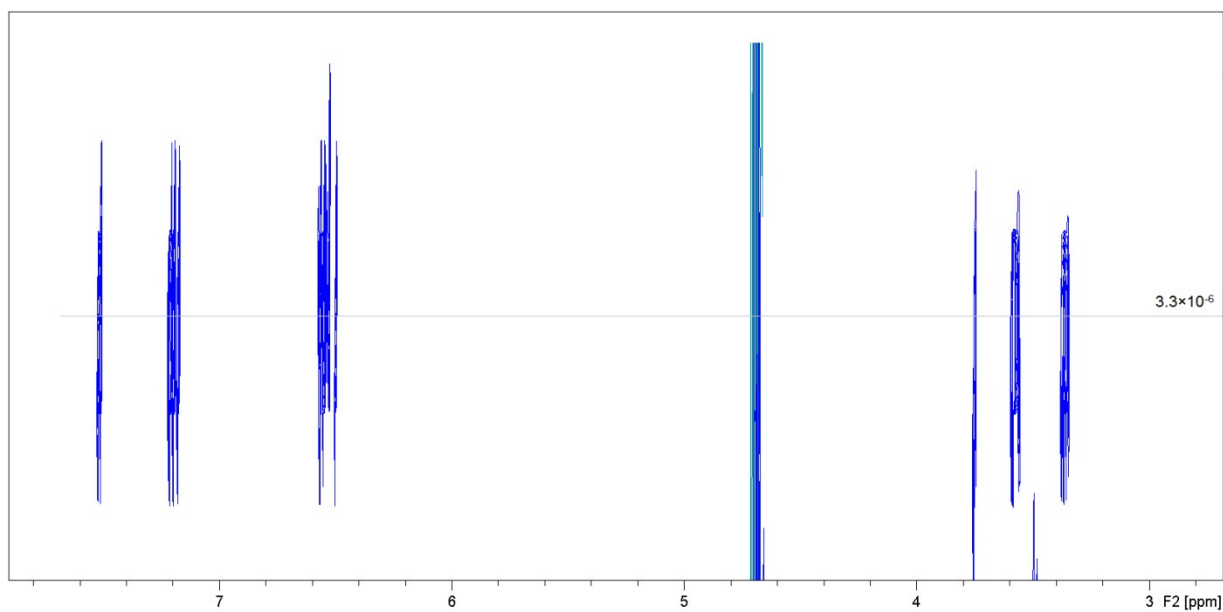


**Figure S17.** 600 MHz DOSY of **L** in 10mM phosphate buffer:D<sub>2</sub>O 9:1 (pH=7.0).

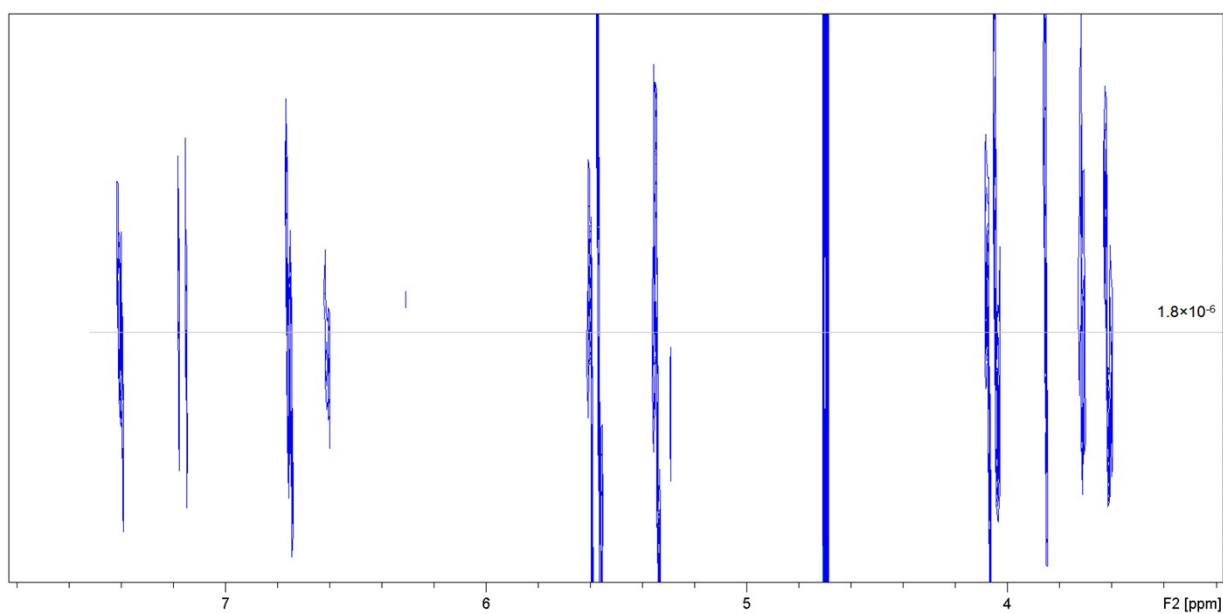


**Figure S18.** 600 MHz DOSY of **L-CB[7]** (1:2) mixture in 10mM phosphate buffer:D<sub>2</sub>O 9:1 (pH=7.0).

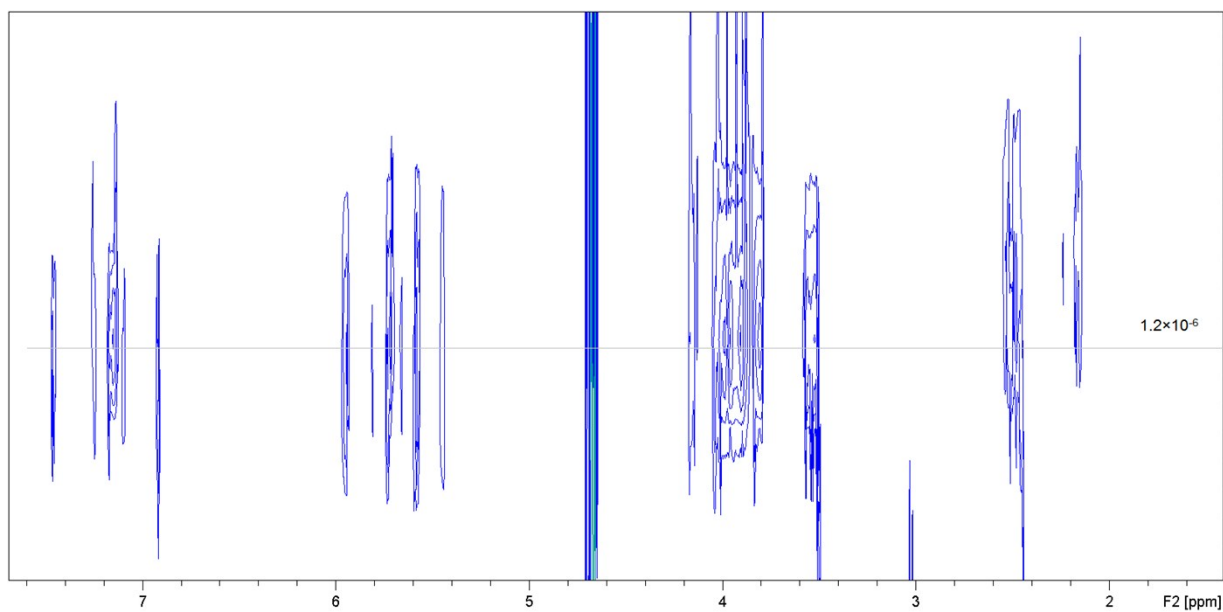


**Figure S19.** 600 MHz DOSY of L-DD (0.3-1) mixture in 10mM phosphate buffer:D<sub>2</sub>O 9:1 (pH=7.0).

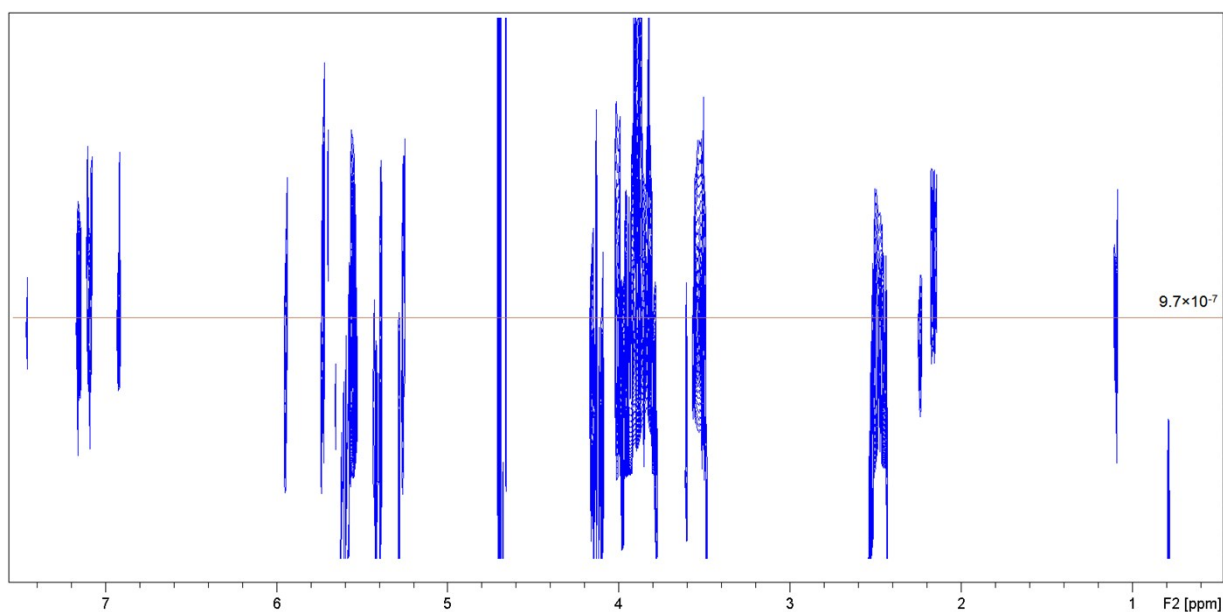


**Figure S20.** 600 MHz DOSY L-DD-CB[7] mixture (1:1.5:3) in 10mM phosphate buffer:D<sub>2</sub>O 9:1 (pH=7.0).

## 5. References

(1) Usoltsev, A. N. et al. (2018) Mononuclear bromotellurates (IV) with pyridinium-type cations: Structures and thermal stability. *Polyhedron* 151, 498-502.